MICHIGAN STATE UNIVERSITY

CYCLOTRON LABORATORY

THE $^{29}Si(^{3}He,p)^{31}P$ REACTION

H. NANN, B.H. WILDENTHAL, H.H. DUHM and H. HAFNER

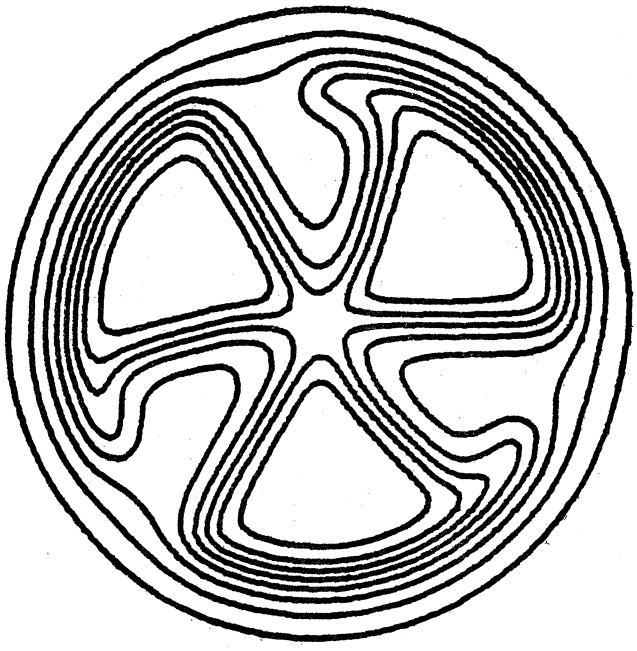

MSUCL-159 FEBRUARY 1975

The $^{29}Si(^{3}He,p)^{31}P$ Reaction

H. Nann

Institut für Kernphysik[+] der J.W. Goethe, Universität, Frankfurt/M, Germany

and

Cyclotron Laboratory[++] and Department of Physics, Michigan State University, East Lansing, Michigan 48824*

and

B.H. Wildenthal

Cyclotron Laboratory[++] and Department of Physics Michigan State University, East Lansing, Michigan 48824

and

H.H. Duhm and H. Hafner
Max-Planck-Institut für Kernphysik, Heidelberg, Germany

ABSTRACT

Angular distributions of the $^{29}Si(^{3}He,p)^{31}P$ reaction at $E_{^3He}$=26 MeV have been measured for states in ^{31}P up to an excitation energy of 5.7 MeV. These data were analyzed with distorted-wave Born approximation calculations based on current shell-model wave functions.

NUCLEAR REACTIONS: $^{29}Si(^{3}He,p)$, E=26 MeV, measured $\sigma(\theta,E_p)$; enriched target; DWBA-analysis.

---

* Present address.

+ Research supported by the Bundesministerium für Forschung und Technologie of Federal Republic of Germany.

++ Research supported in part by the U.S. National Science Foundation.

I. INTRODUCTION

The present investigation of the $^{29}Si(^{3}He,p)^{31}P$ reaction is part of a systematic study of two-nucleon transfer reactions on 2s-1d shell nuclei[1]. A major aim of this study is to provide a critique of existing nuclear structure theory from the standpoint of the matrix elements of the coupled two-particle creation operator. The comparison of experimental differential cross sections with the results of microscopic distorted-wave Born approximation (DWBA) calculations based upon the matrix elements $\langle\psi(A+2)|[a^+(n_1\ell_1j_1)\ a^+(n_2\ell_2j_2)]_{J,T}\ |\psi(A)\rangle$ can provide discriminating tests of the wave functions $\psi(A+2)$ and $\psi(A)$[2,3].

In this paper we present measured angular distributions for transitions to levels of ^{31}P in the region of excitation energy from 0 to 5.7 MeV. The experimental data for the states of well established spin and parity, J^π, are compared with DWBA calculations based on the shell-model wave functions of Wildenthal, et al.[4,5] These wave functions are obtained in a truncated $(1d_{5/2})^{n_1}(2s_{1/2})^{n_2}(1d_{3/2})^{n_3}$ vector space of all $n_1 \geq 9$ configurations plus the $n_1=8$, $n_2=4$, $n_3=1$ configuration for the ^{29}Si ground state[4]) and of all $n_1 \geq 10$ configurations for the levels of ^{31}P. [ref. 5)]. The modified surface delta interaction MSDI was used as the effective two-body interaction in these shell model calculations.

II. EXPERIMENTAL PROCEDURE AND RESULTS

The experiment was performed with a 26 MeV ^{3}He-beam from the MP tandem Van de Graaff accelerator at the Max-Planck-Institut für Kernphysik in Heidelberg. The target was a self-supporting SiO foil, enriched to 98% in ^{29}Si. It was fabricated by vacuum evaporation of SiO_2 onto a glass slide, the SiO_2 being reduced to SiO by means of Ta-powder as part of the evaporation process. The measured areal density of the ^{29}Si target was about 70 μg/cm^2. During the experiment the target thickness was monitored by recording elastically scattered ^{3}He particles at a fixed angle. The emergent protons were detected in 50 μm Ilford L-4 nuclear emulsions after being momentum analysed in a multigap magnetic spectrograph. The emulsion plates were covered with absorbing foils of polyethylene and copper in order to stop other impinging particles.

Proton spectra were recorded from 5.5° to 88° in steps of 3.5°. An energy resolution (FWHM) of about 40-45 keV was obtained. A spectrum at an angle of 17° is shown in fig. 1. Groups corresponding to states in ^{31}P are labelled by their excitation energy. The extracted angular distributions for the transitions to levels in ^{31}P up to an excitation energy of 5.7 MeV are shown in figs. 2 and 3. The error bars shown on the experimental data points represent the relative errors. The absolute cross section scale was established by measuring the elastic scattering of protons at 1.92 MeV on the ^{29}SiO target, and is believed accurate to ±20%.

III. DISTORTED WAVE ANALYSIS

The calculations of the theoretical differential cross sections were carried out with the DWBA code DWUCK[6]). The form factors were calculated separately by the method of Drisko and Rybicki[7]) using a modified version of the code FOCAL[8]) and were fed into DWUCK as data. Details of the present method for the DWBA analysis have been described in previous papers[1]). The optical potentials which were used for calculating the distorted waves in the entrance and exit channels were adapted from the literature[9,10]) and are given in table 1. Spin-orbit dependent distortions were neglected in order to permit the sum over the transferred angular momentum L and spin S in the transition amplitude to be incoherent. No lower cut-off in radial integration was employed. The spectroscopic amplitudes for the various transitions analysed were calculated from wave functions of ref. [4,5])and are listed in table 2.

The calculated differential cross sections for the transitions to those positive parity states which could be presumed to correspond to states obtained in the shell-model calculations described above are compared in fig. 2 with the experimental data. Fig. 3 displays miscellaneous other (^{3}He,p) angular distributions. As shown in figs. 2 and 3, each calculated angular distribution is independently normalized for a best fit to the experimental data. From these fits, the ratios between experimental and calculated cross sections were determined and listed in table 3. For the theoretical cross sections

an empirical normalization factor $D_o^2=22 \times 10^4$ MeV^2 fm^3 was used. A similar value ($D_o^2=25 \times 10^4$ MeV^2 fm^3) has been reported by Casten et al.[11] for (t,p) reactions on Pb, Sn, Zr and Ca isotopes. It should be noted that this empirical over-all normalization factor is quite sensitive to the mass-3 optical model parameters, especially to the depth of the real and imaginary potential. The values mentioned above hold only for the depths of the real potential of ∿170 MeV and of the imaginary potential of ∿20 MeV. In table 3, values given in brackets indicate that the shape of the angular distribution is not even approximately reproduced by the calculations. A ratio between experimental and theoretical cross sections of unity presumably corresponds to a good agreement between experiment and theory. Hence, the overall success of the shell-model wave functions lies in the consistency with which this ratio remains close to unit for many states.

IV. DISCUSSION

According to the simple shell model, the main component of the ^{29}Si ground state is $(^{16}O)(1d_{5/2})^{12}(2s_{1/2})^1$. Thus, in the ^{29}Si(^{3}He,p) reaction, states in ^{31}P with $J^\pi \leq 7/2^+$ should be predominantly populated by transferring the proton-neutron pair in the $(2s_{1/2})^2$, $(2s_{1/2},1d_{3/2})$ and/or $(1d_{3/2})^2$ configurations. The population of states with $J^\pi \geq 9/2^+$ is determined by the fraction of $(1d_{5/2})$ holes in the wave functions, since these states can only be connected by transfer involving $1d_{5/2}$ particles, assuming the exclusion of first-order contributions from higher major shells.

4.1 Transitions to the $1/2^+$ states at 0.00, 3.14 and 5.25 MeV.

The (^{3}He,p) selection rules allow a mixture of L=0 and L=2 for $1/2^+ \rightarrow 1/2^+$ transitions. The L=2 admixture is allowed only if the proton pair is transferred with the quantum numbers (J,T)=(1,0). Assuming equal spectroscopic amplitudes, the cross sections for pure transfer of proton-neutron pairs coupled to (J,T)=(1,0) and L=2 in the allowed configurations are proportional to the following values: $(2s_{1/2}, 1d_{3/2})$= 1.0, $(1d_{3/2})^2$ =0.17, $(1d_{5/2},1d_{3/2})$= 0.08 and $(1d_{5/2})^2$= 0.05. Accordingly, the $(2s_{1/2},1d_{3/2})$ spectroscopic amplitudes gives by far the largest L=2 contribution.

The experimental angular distributions to the 0.00 and 5.25 MeV states exhibit predominantly L=0 patterns (see fig. 2), whereas the transition to the 3.14 MeV state shows a considerable L=2 admixture. The wave functions used in the present analysis yield "pure" L=0 angular distributions for the first and second $1/2^+$ states in the theoretical spectrum, an L=2 distribution for the third and a weak L=0 distribution for the forth state. Thus, noting the normalization factor for the ground state transition of 0.9 in table 3, we see that the theory yields a good account for the experimentally observed shape and strength of the ground state transition. For the transition to the second experimentally known $1/2^+$ state at 3.14 MeV, the L=2 contribution is by far underestimated; the major spectroscopic amplitudes (see table 2) for this transition contribute by destructive interference to the L=0 component and by constructive interference to the L=2 component of the differential cross section. In addition, the spectroscopic amplitude of the

intrinsically strong $(2s_{1/2},1d_{3/2})$ configuration is quite small (see table 2) and interferes destructively with $(1d_{3/2})^2$, the major spectroscopic amplitude.

There are two theoretical states which may possibly correspond to the experimental $1/2^+$ state at 5.25 MeV. These theoretical states, the third and fourth in the theoretical spectrum, have calculated energies of 3.97 and 5.01 MeV. The wave function of the third theoretical $1/2^+$ state yields an L=2 calculated shape (full line in fig. 2) in clear disagreement with the experimental data. The wave function of the fourth theoretical $1/2^+$ state yields an L=0 calculated shape (dotted line in fig. 2) which agree with the observed shape of the 5.25 MeV angular distribution. Even so, the agreement in magnitude between the calculated intensity of the fourth $1/2^+$ transition and the observed level at 5.25 MeV is not good enough for an unambiguous correspondence to be demonstrated.

4.2 Transitions to the $3/2^+$ states at 1.27, 3.51 and 4.26 MeV.

The selection rules for a (^{3}He,p) reaction permit a mixture of L=0 and L=2 transfer for $1/2^+ \rightarrow 3/2^+$ transitions. Nearly pure L=2 patterns are observed for the transitions to the first and third $3/2^+$ states at 1.27 and 4.26 MeV excitation, whereas a mixture of L=0 and L=2 shapes are observed for the transition to the second $3/2^+$ state at 3.51 MeV excitation. The shell-model wave functions used in the present analysis yield "pure" L=2 angular distributions for the first and second $3/2^+$ states in the theoretical spectrum and a mixture of L=0 and L=2 for the third

state. Thus the shape of the transition to the 1.27 MeV state is well accounted for by the theory. Noting the normalization factor of 1.27 in table 3, the magnitude of the differential cross section is also well described. The predictions for the second and third $3/2^+$ states are in clear disagreement with the experimental data. Qualitatively, an agreement in shapes is obtained by postulating an inversion in energy of the second and third states in the theoretical spectrum such that the third theoretical $3/2^+$ state corresponds to the 3.51 MeV experimentally observed state and the second theoretical $3/2^+$ state to the 4.26 MeV experimentally observed state. Furthermore, the magnitude of the differential cross section for the 4.26 MeV transition would then be well accounted for, although this would not be the case for the 3.51 MeV transition. Another complication in the interpretation of the results for the 3.51 MeV state arises from the possibility that this level is actually a $3/2^+$-$1/2^+$ doublet, as suggested by Wolff and Leighton[12]). If this were the case, the third theoretical $1/2^+$ state would perhaps correspond to the one member of this doublet. The angular distribution for this third theoretical $1/2^+$ state, however, exhibits a "pure" L=2 pattern (see previous subsection) and thus would still not provide an account for the experimentally observed L=0 admixture in the 3.51 MeV differential cross section.

4.3 Transitions to the $5/2^+$ states at 2.23, 3.30, 4.19, 4.78 and 5.12 MeV.

These $5/2^+$ states can be populated in principle by both L=2 and L=4 transfer components. The experimental angular distributions are predominantly L=2 for the 2.23, 3.30, 4.19 and 4.78 MeV states (see fig. 2) and L=4 for the 5.12 MeV transition (see fig. 3). The first four $5/2^+$ states can be identified with the first four shell-model states. The wave functions in each case yield "pure" L=2 angular distributions in agreement with the experimental data. Consideration of the relative strengths show that only the magnitude of the fourth, 4.78 MeV, state is well predicted. The calculated magnitudes for the transitions to the first, second and third $5/2^+$ states are each off by factors of more than 2 from the observed strengths. An energy inversion in the theoretical spectrum of the first and second $5/2^+$ states would alter the situation so as to produce quite a good account of the experimental differential cross sections of the 2.23 and 3.30 MeV transitions (see table 3). Such an inversion of the $5/2^+$ levels would, however, be qualitatively inconsistent with the observed $1d_{5/2}$ single nucleon pick-up spectroscopic factors in the $^{32}S(d,^3He)^{31}P$ reaction[13]). It appears therefore that the shell-model wave functions for the $5/2^+$ states fail to correctly account in general for the details of configuration mixing and $1d_{5/2}$ hole strength.

For the fifth experiment $5/2^+$ state at 5.12 MeV no shell-model wave functions are available. The observed angular distribution is nicely fitted by a pure L=4 calculation assuming a $(1d_{3/2})^2_{3,0}$ transfer, as it is shown in fig. 3. Since this transfer component produces the by far largest L=4 contribution [see ref.[1])] one can suggest that the wave function for the fifth $5/2^+$ state should contain a large $(2s_{1/2})^1\ (1d_{3/2})^2_{3,0}$ component.

4.4 Transitions to the $7/2^+$ state at 3.41 MeV and to the $9/2^+$ state at 5.34 MeV.

The $7/2^+$ level at 3.41 MeV is observed to be populated with a predominant L=4 angular distribution (see fig. 2), although an L=2 admixture which is kinematically enhanced over the L=4 component is allowed by the selection rules. The shell-model wave function of the first $7/2^+$ state predicts a dominant L=2 angular distribution with some L=4 admixture, thus not reproducing the experimental data. Beyond that, the magnitude of the differential cross section is underestimated by more than a factor of 3.

The transition to the $9/2^+$ state at 5.34 MeV can proceed only by a L=4 transfer. Here the quantative nuclear structure information available from the data is contained only in the transition strength. The wave function of the first $9/2^+$ model state over-predicts the magnitude of the differential cross section by nearly a factor of 2. This suggests that the number of $(1d_{5/2})$ holes in the shell-model wave function of this state is underestimated, a feature which seems to be a consequence of the truncation of the configuration space.

4.5 Miscellaneous other transitions.

For the $^{30}Si(^{3}He,d)^{31}P$ reaction Wolff and Leighton[12]) observed strong ℓ=3 and ℓ=1 spectroscopic factors for the transitions to the $7/2^-$ state at 4.43 MeV and to the $3/2^-$ state at 5.01 MeV, respectively, leading to the conclusion that these two states have rather pure single-particle character. Since the main component of the ^{29}Si ground state is $(2s_{1/2})^1$, the $7/2^-$ state can then be populated by $(2s_{1/2},1f_{7/2})$ transfer and the $3/2^-$ state by $(2s_{1/2}, 2p_{3/2})$ transfer resulting in L=3 and L=1 angular distributions, respectively. In fig. 3 these L=3 and L=1 angular distributions are shown superimposed on the experimental data. The angular dependence of the differential cross section is quite well reproduced, indicating that in the case of the 5.01-5.02 MeV doublet the contribution from the other members to the summed cross section is comparatively small.

The transition to the 4.59-4.63 MeV and 5.53-5.56 MeV doublets could not be experimentally resolved under each angle. Both doublets contain $J^\pi=3/2^+$ and $J^\pi=7/2^+$ members. Their experimentally observed angular distributions are very similar showing a large L=4 component and a forward angle peaking characteristic to a L=0 component. The L=4 component can be attributed to the $7/2^+$ member whereas the L=0 component to the $3/2^+$ member.

V. CONCLUSIONS

In the present paper we have attempted to reproduce the experimental differential cross section of the $^{29}Si(^{3}He,p)^{31}P$ reaction with microscopic DWBA calculations based on available shell-model wave functions. Only the transitions observed to the first $1/2^+$ and $3/2^+$ states in ^{31}P are well accounted for by the calculations. For the higher lying $1/2^+$ and $3/2^+$ states the correspondence between experimental levels and model states deteriorates, since in many cases the higher lying model state seem to show features of the lower lying experimental level. The failure of the shell-model calculations in describing the transitions to the $5/2^+$ states--the agreement for the fourth $5/2^+$ state should probably be considered accidental--may point to the need of an extension of the configuration space to more than two $1d_{5/2}$ holes. A further indication that the omission of some $1d_{5/2}$ hole configurations in the active shell-model space is a significant deficiency comes from the transition to the first $9/2^+$ state, where the magnitude of the theoretical differential cross section is overestimated, since $9/2^+$ states in ^{31}P can only be constructed upon $(1d_{5/2})$-hole configurations in ^{29}Si.

ACKNOWLEDGEMENTS

One of the authors (H.N.) would like to thank Profs. P. Brix, W. Gentner and U. Schmidt-Rohr for the hospitality at the Max-Planck-Institut für Kernphysik in Heidelberg.

REFERENCES

1. H. Nann, B. Hubert and R. Bass, Nucl. Phys. A176 (1971)533; B. Hubert, H. Nann, W. Schäfer and R. Bass, Nucl. Phys. A181 (1972)1; H. Nann, T. Mozgovoy, R. Bass and B.H. Wildenthal, Nucl. Phys. A192, (1972)417; H. Nann, L. Armbuster and B.H. Wildenthal, Nuc. Phys. A198 (1972)11.
2. I.S. Towner and J.C. Hardy, Adv. in Phys. 18 (1969)401.
3. W.G. Davies, J.C. Hardy and W. Darcey, Nucl. Phys. A128 (1969)465.
4. B.H. Wildenthal and J.B. McGrory, Phys. Rev. C7 (1973)714.
5. B.H. Wildenthal, J.B. McGrory, E.C. Halbert and H.D. Graber, Phys. Rev. C4 (1971)1708.
6. P.D. Kunz, University of Colorado, private communication.
7. R.M. Drisko and F. Rybicki, Phys. Rev. Lett. 16 (1966)275.
8. F. Pühlhofer, Nucl. Phys. A116 (1968)516, and private communication.
9. G.W. Greenlees and G.J. Pyle, Phys. Rev. 149 (1966)836.
10. H.P. Morsch and R. Santo, Nucl. Phys. A179 (1972)401.
11. R.F. Casten, E.R. Flynn, O. Hansen and T.J. Mulligan, Phys. Rev. C4 (1971)130.
12. A.C. Wolff and H.G. Leighton, Nucl. Phys. A140 (1970)319.
13. G.T. Kashl, G. Mairle, U. Schmidt-Rohr and G.J. Wagner Nucl. Phys. A136 (1969)286.
14. P.M. Endt and C. van der Leun, Nucl. Phys. A214 (1973)1
15. P.J. Twin, E.M. Jayasinghe, G.D. Jones, P.R.G. Lornie,

FIGURE CAPTIONS

Fig. 1.--Proton spectrum from the $^{29}Si(^{3}He,p)^{31}P$ reaction.

Fig. 2.--Angular distributions of the $^{29}Si(^{3}He,p)^{31}P$ reaction. The curves correspond to DWBA calculations. For further explanations see text.

Fig. 3.--Proton angular distributions for miscellaneous levels in ^{31}P. The curves are DWBA fits to the data.

Table 1.--Optical-model parameters used in the DWBA calculations.

	V (MeV)	W_v (MeV)	W_s (MeV)	r_o (fm)	a (fm)	r_c (fm)	r_I (fm)	a_I (fm)
^{3}He	173.9	20.6		1.15	0.72	1.40	1.50	0.82
p	45.5		13.0	1.20	0.70	1.25	1.25	0.70

The ^{3}He-parameters are adapted from ref. 10, the p-parameters from ref. 9.

Table 2.--Spectroscopic amplitudes for the $^{29}Si(^{3}He,p)^{31}P$ reaction.

J_B	T_B	E_x^{th} (MeV)	(J,T)	(D5,D5)	(S1,S1)	(D3,D3)	(D5,S1)	(D5,D3)	(S1,D3)
$1/2^+$	1/2	0.00	0 1	.4319	.7789	.5389			
			1 0	-.1759	-.7284	.1538		-.1529	-.0110
		3.63	0 1	.0463	.4257	-.5306			
			1 0	-.0948	-.4761	-.2259		.1319	-.0777
		3.97	0 1	.0073	.0552	-.0235			
			1 0	.0785	-.0642	-.3466		-.0408	.4399
		5.01	0 1	.0486	.1378	-.3923			
			1 0	-.0464	-.0825	.4733		-.1304	.1004
$3/2^+$	1/2	1.23	1 0	-.0821	-.0133	.2343		.0438	-.5584
			2 1	-.0008		.1938	-.0698	-.0349	.4309
			2 0				-.0118	-.0624	.4888
		3.93	1 0	.0455	.0225	-.1816		-.0331	.1478
			2 1	-.0386		-.1772	-.0460	.0388	-.3193
			2 0				.1044	-.0402	.5231
		4.55	1 0	.0506	.0154	-.2147		-.0844	.0665
			2 1	-.0291		.2500	-.0058	.1594	-.0725
			2 0				-.0467	.0185	-.0379
$5/2^+$	1/2	2.48	2 1	-.0417		.0364	-.0994	.0311	.3106
			2 0				.0713	-.0908	-.1839
			3 0	.0751		-.0147	.2255	.0630	
		2.84	2 1	-.0598		-.2975	-.0089	.0563	-.7520
			2 0				.0334	-.1059	.4294
			3 0	.0050		-.0468	-.1504	.0937	
		4.70	2 1	.0380		-.3983	.0549	-.1165	.2276
			2 0				-.0366	.0415	-.1322
			3 0	-.0191		-.2755	-.0915	.1540	
		4.91	2 1	-.0504		-.3619	-.1374	.0867	.0310
			2 0				.0523	-.0382	-.0227
			3 0	.0386		-.2062	.1525	.0845	

Table 2.--Cont.

J_B	T_B	E_x^{th} (MeV)	(J,T)	(D5,D5)	(S1,S1)	(D3,D3)	(D5,S1)	(D5,D3)	(S1,D3)
$7/2^+$	1/2	3.65	3 0	-.0281		.2197	-.0497	.1254	
			4 1	.0286				-.0908	
			4 0					-.1117	
$9/2^+$	1/2	5.02	4 1	-.0129				-.1386	
			4 0					+.0719	
			5 0	-.4600					

Table 3.--Comparison of experimental and theoretical cross sections.

E_x^{exp} (MeV)	J^π	E_x^{th} (MeV)	σ_{exp}/σ_{th}
0.00	$1/2^+$	0.00	0.91
1.27	$3/2^+$	1.23	1.27
2.23	$5/2^+$	2.48	3.54
		2.84	1.14
3.13	$1/2^+$	3.63	(2.09)
3.30	$5/2^+$	2.84	0.45
		2.48	1.36
3.41	$7/2^+$	3.65	(3.64)
3.51	$3/2^+$	3.93	(0.91)
		4.55	9.10
4.19	$5/2^+$	4.70	2.32
4.26	$3/2^+$	4.55	(8.65)
		3.93	1.09
4.78	$5/2^+$	4.91	0.78
5.25	$1/2^+$	3.97	(1.10)
		5.01	7.28
5.34	$9/2^+$	5.02	0.48

Excitation energies are taken from ref. 14, the spin and parity assignments from ref. 15.

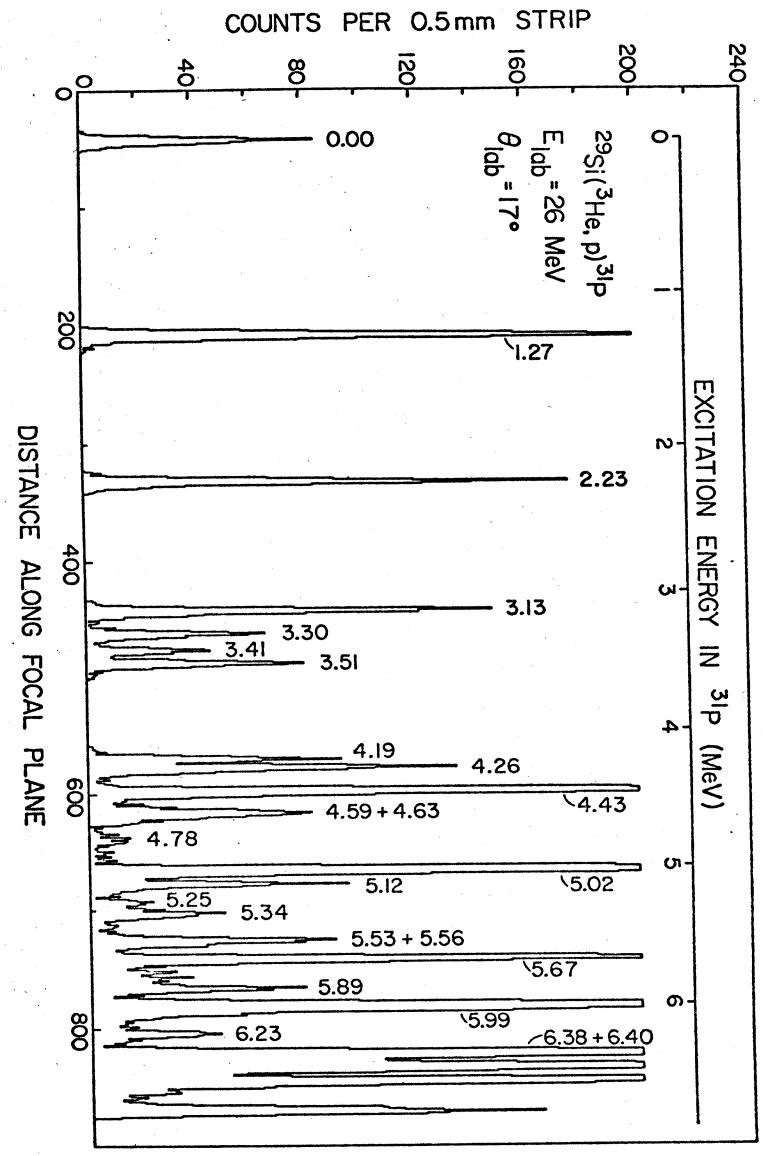

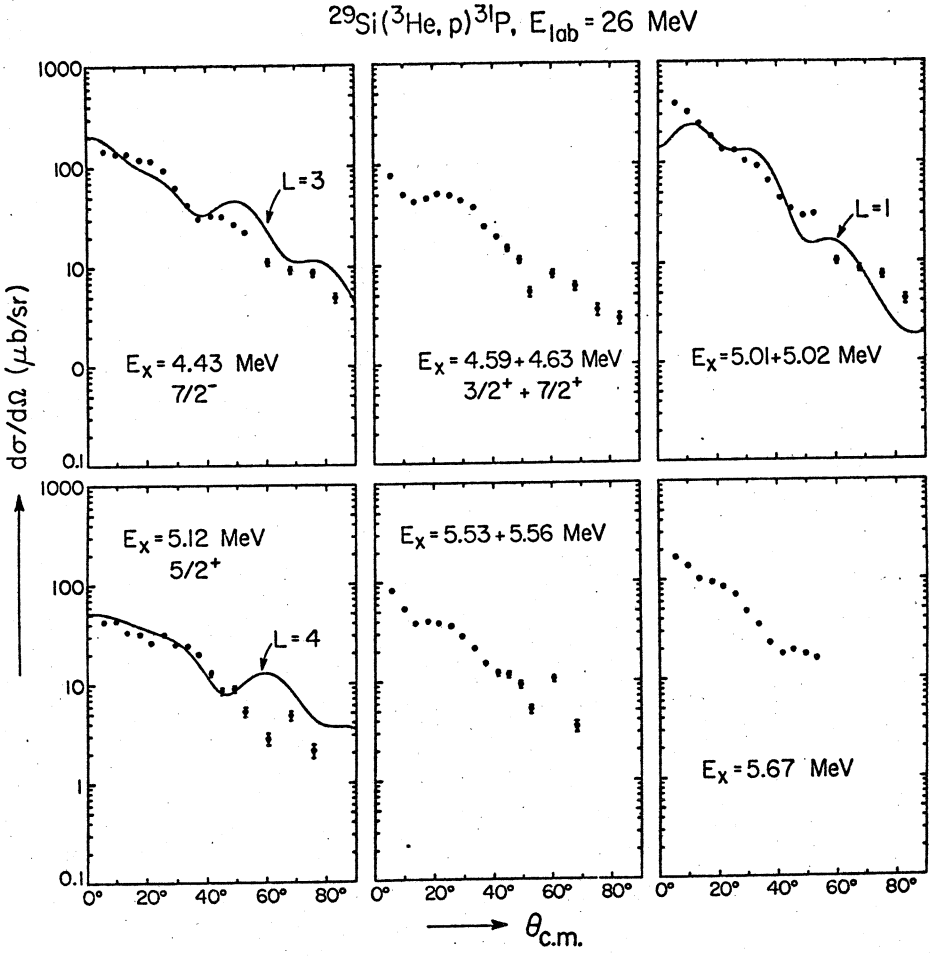
$^{29}Si(^3He, p)^{31}P$, E_{lab} = 26 MeV
$d\sigma/d\Omega$ (μb/sr)
E_x = 4.43 MeV
7/2$^-$
L=3
E_x = 4.59+4.63 MeV
3/2$^+$ + 7/2$^+$
E_x = 5.01+5.02 MeV
L=1
E_x = 5.12 MeV
5/2$^+$
L=4
E_x = 5.53+5.56 MeV
E_x = 5.67 MeV
$\theta_{c.m.}$

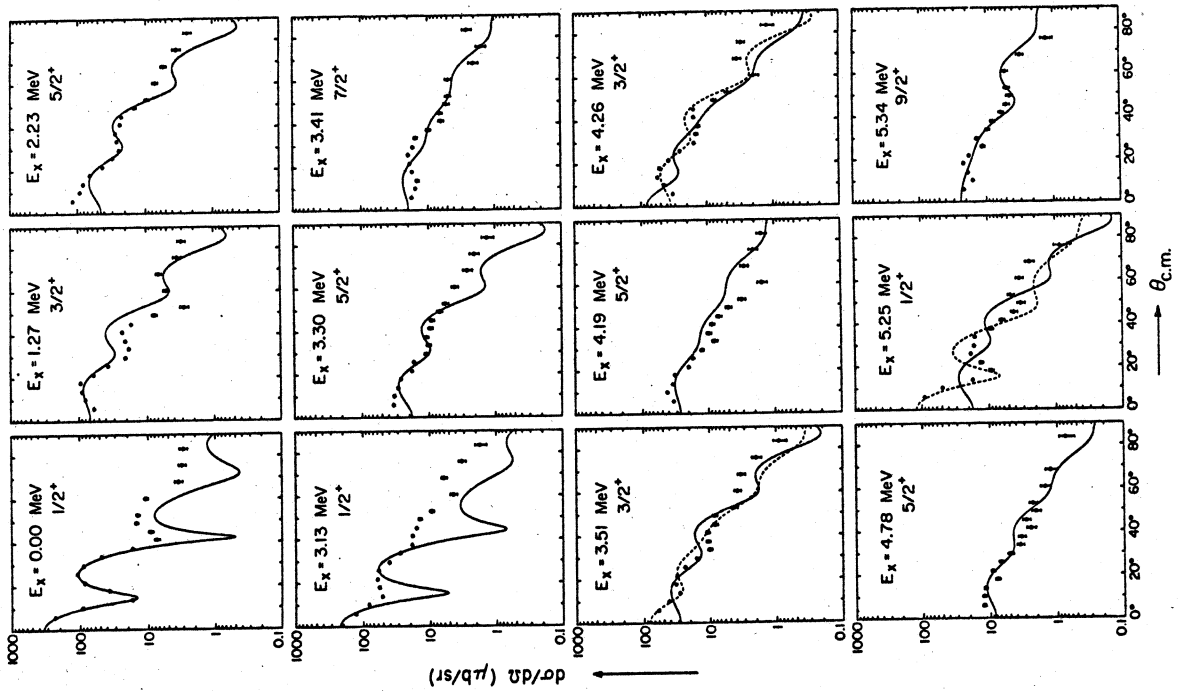
E_x = 0.00 MeV 1/2$^+$
E_x = 1.27 MeV 3/2$^+$
E_x = 2.23 MeV 5/2$^+$
E_x = 3.13 MeV 1/2$^+$
E_x = 3.30 MeV 5/2$^+$
E_x = 3.41 MeV 7/2$^+$
E_x = 3.51 MeV 3/2$^+$
E_x = 4.19 MeV 5/2$^+$
E_x = 4.26 MeV 3/2$^+$
E_x = 4.78 MeV 5/2$^+$
E_x = 5.25 MeV 1/2$^+$
E_x = 5.34 MeV 9/2$^+$
$d\sigma/d\Omega$ (μb/sr)
$\theta_{c.m.}$